Fermi National Accelerator Laboratory

FERMILAB-FN-628

The MARS Code System User's Guide Version 13(95)

Nikolai V. Mokhov

Fermi National Accelerator Laboratory
P.O. Box 500, Batavia, Illinois 60510

April 1995

Operated by Universities Research Association Inc. under Contract No. DE-AC02-76CHO3000 with the United States Department of Energy

Disclaimer

The MARS Code System User's Guide Version 13(95)

Nikolai V. Mokhov

Fermi National Accelerator Laboratory

P.O. Box 500, Batavia, Illinois 60510

April 25, 1995

Abstract

This paper is a user's guide to the current version of the MARS Monte Carlo code. MARS performs fast inclusive simulations of three-dimensional hadronic and electromagnetic cascades, muon and low energy neutron transport in shielding and in accelerator and detector components in the energy range from a fraction of an electronvolt up to 30 TeV. The code has undergone substantial improvements since the last documented version MARS10 and all these as well as other specific features of the MARS code system are explained in detail. Descriptions of general input and output with commentary and recomendations are given. Examples are given for running the program with distributed sources, complex compounds, arbitrary geometries, and magnetic fields. Use of the code in a multistage mode, coupled with event generators (DTUJET), with the STRUCT program for tracking particles in accelerator lattices with beam loss recording, and with physics analysis and graphics packages is demonstrated with typical input and output examples.

Contents

1 Introduction 3

2 MARS System 4
- 2.1 Base . . . 4
- 2.2 Major Features . . . 5
- 2.3 Structure . . . 8
- 2.4 MAIN Example . . . 10
- 2.5 Usage . . . 11

3 General Input 11
- 3.1 Framework . . . 11
- 3.2 Card Input Sequence (MARS.INP) . . . 13
- 3.3 Extended Geometry (GEOM.INP) . . . 21
- 3.4 Materials, Defaults and Energy Groups . . . 23
- 3.5 Input Examples . . . 26

4 User Subroutines 28
- 4.1 Compounds (MIXTUR) . . . 28
- 4.2 Source (BEG1) . . . 29
- 4.3 Geometries (REG1, REG2, REG3) . . . 30
- 4.4 Magnetic and Electrical Fields (FIELD, SUFI) . . . 33
- 4.5 Leakage (LEAK) . . . 34
- 4.6 Fictitious Scattering (ALIGN, SAGIT) . . . 35
- 4.7 Edge Scattering (EDGEUS) . . . 36
- 4.8 Special Volumes (VFAN) . . . 37
- 4.9 Intermediate Dumps (DUMP) . . . 37

5 Output 38
- 5.1 General Output (MARS.OUT) . . . 38
- 5.2 Histograms . . . 42

6 Physics Analyses: Examples 43

7 Rules-Of-Thumb 49

8 Acknowledgements 51

9 References 52

1 Introduction

The MARS code system is a set of Monte Carlo programs for inclusive simulation of three-dimensional hadronic and electromagnetic cascades in matter, of muon and low-energy neutron production and transport in radiation shielding, accelerator and detector components at energies up to 30 TeV. It allows fast cascade simulation with modest memory requirements in complex geometries with composite materials, in presence of arbitrary magnetic fields, with a variety of variance reduction techniques, other optimization and scoring options.

The MARS code has undergone substantial improvements since the last documented version MARS10 [1]. The purpose of this document is to be a user's guide for a new MARS, version 13(95), so the paper reproduces the needed sections of the previous manual with a detailed description of all the main improvements and additional options. The main changes compared to MARS10 and to MARS12 released in 1992 [2], concern the hadron production model, muon and low-energy neutron production and transport, photo-hadron and photo-muon production, e^+, e^-, γ and hadron production by muons, synchrotron radiation, muon decays, precise particle tracking in a magnetic field, extended geometry module, radioactivation calculation, computing performance, complete double precision mode, new input and output with significantly extended scoring and visualization capabilities. If needed, the code couples to the DTUJET event generator [3] and to the STRUCT code for multi-turn particle tracking in an accelerator lattice [4]. By 1995 there are about 50 MARS users worldwide.

2 MARS System

2.1 Base

Feynman's ideas concerning an inclusive approach to multiparticle reactions [5] and a biasing techniques served as a basis for the original program MARS [6] as well as for the program CASIM [7]. To construct a cascade tree only a fixed number of particles from each vertex is chosen (depending on the problem considered) and each carries a statistical weight which is equal, in the simplest case, to the partial mean multiplicity of the particular event. Energy and momentum are conserved on the average over a number of collisions. The practical reasons for the inclusive scheme as described in [8, 9, 10, 11] are:

- CPU time per incident particle grows only logarithmically with incident energy, compared to the linear rise in the exclusive mode, which allows the easier simulation of multi-TeV cascades;
- in many applications one considers effects due to the simultaneous interactions of a huge number of particles, so to describe the cascade it is sufficient to obtain the first moment of the distribution function using the inclusive cross-sections, in the same manner as with Boltzman's equation;
- experimental data on inclusive spectra are more readily available than on exclusive ones;
- the use of statistical weights allows the production of a given particle type to be enhanced within the phase-space region of interest, especially for rarely produced particles.

A disadvantage of this approach is the impossibility of directly studying fluctuations from cascade to cascade. Other codes have in the meantime adopted a similar approach to simulate very high energy electromagnetic[12] and hadronic[13] showers.

The mathematical foundation and the physical model of the MARS system as well as benchmarks for numerous applications are described in detail in [2, 9, 11, 14, 15]. The program has been developed over many years. Besides the original version [6] the milestones were: MARS3 [16], MARS4 [17], MARS6 [18], MARS8 [19], MARS9 [20], MARS10 [1, 21], MARS12 [2, 22], MARS93 [23], the hydrodynamical MARS/MESA/SPHINX package [24] and a parallel version of MARS12 [25].

2.2 Major Features

The main features of the MARS code system, version 13(95), in physics, geometry and analysis/computing categories are listed here.

1. **Physics Model:**

   - all interactions of hadrons, leptons and photons during their passage through matter are taken into account for the energy range from 30 TeV down to about 0.2 MeV (0.00215 eV for neutrons);
   - each hA vertex is constructed in a problem-oriented way from a simplest case with one or two hadrons in the final state (e.g., leading particle bias), through the analog (exclusive) type vertex, to the sophisticated cases with enhancements in phase-space and/or particle type (e.g., $\tilde{p}$ production [15, 26]);
   - simulation of hadron-nucleus interactions at $E \geq 5$ GeV is based on a set of the semi-theoretical formulas for a proton target, coupled with the additive quark model of hadron-nucleus interactions for fast secondaries and phenomenological model for slow particles [11, 14, 27, 28, 29, 30, 31]; production of diffractive particles and nuclear de-excitation processes are modeled separately; at $E \leq 5$ GeV, hadron-nucleus inelastic collisions are simulated using modified formulas [32]; special treatment was added in the new version to provide better energy balance;
   - optional coupling with DTUJET [3] event generator for primary high energy pp– or $\tilde{p}p$–collisions [33, 34];
   - hadron-nucleus inelastic cross-sections are calculated for a set of nuclei in the framework of the optical model and tabulated in the energy range from 10 MeV to 30 TeV for subsequent interpolation [11, 35];
   - interactions and transport of neutrons in the 0.00215 eV to 14.5 MeV energy range (see Table 7 of Sect. 3.4) is performed using 28-group library BNAB [36] in the P_5-approach [22] with a special treatment for very extended systems like multi-section labyrinths [37, 38]; optional is 49-group library for neutrons below 18 MeV (see Table 8), married with 15-group system for secondary photons in the 10 keV to 11 MeV energy range (Table 9) [23, 36];

- special attention is paid to processes with a small momentum transfer: multiple Coulomb scattering using Moliere's theory with allowance for nuclear size effects, elastic scattering, diffraction, δ-rays and direct e^+e^- production by hadrons [9, 20, 35, 39, 40];
- fast precise algorithm for simulation of ionization energy loss [35, 41];
- edge scattering with step optimization depending on direction and location of a particle near the surface [22, 42];
- muon production with forced decays of mesons and short-lived resonances [9, 11, 43, 44];
- very efficient algorithms for muon interactions (ionization, bremsstrahlung, direct e^+e^- pair, and deep inelastic) and transport [35] well advanced compared to previous versions [1, 11, 43, 44];
- optional forced $\mu \rightarrow e\nu\tilde{\nu}$ decays and synchrotron radiation generation [45];
- photoneutron production in a giant resonant energy region [22, 46];
- leading particle biased simulation via modified AEGIS code [47] of electromagnetic showers, initiated by π^0 decays, high energy $\delta-$rays, prompt e^+e^- from hadrons, muons and photoneutrons;
- phenomenological algorithm for radionuclide production with a point kernel techniques for gamma dose rate [22].

2. **Geometry, Transport and Materials:**

- iterative step-wise particle tracking with precise localization of boundaries, which is especially refined near matter-vacuum edges [11, 48, 49]; advanced algorithm for tracking in a magnetic field;
- multi-medium multi-component geometrical module with optional superfine structure distributed, if desired, over thousands of meters, in presence of arbitrary magnetic fields;
- optional extended geometry description [50] with allowance for easier handling of an arbitrary combination of boxes, cylinders, spheres and cones with some visualization options;
- 22 materials are built into the code and others can be easily defined by the user; each material can be a mixture of up to 6 chemical elements; up to 20 different materials can simultaneously be involved in a specific calculation;

- fusion with the STRUCT code [4] for multi-turn particle tracking in the accelerator lattice represented by an arbitrary combination of magnetic elements and transfer matricies allowing unified approach to beam loss and radiation effects studies at modern accelerators [40, 48, 51, 52, 53, 54];
- geometry and phase-space tagging options, which allow very efficient way to study a source term;
- variance reduction options: phase-space and particle type biasing, exponential conversion of path length, mathematical expectation, splitting and Russian roulette for particle trajectories and statistical weights [11].

3. **Computing and Analysis:**

   - scoring of three-dimensional distributions of star density, total and partial particle fluences, total and partial energy deposition densities, temperature rise, dose equivalent, residual dose rate; corresponding statistical errors; energy spectra in the predefined regions; tagged distributions and some integral values;
   - substantially extended (compared to the previous versions) histogramming and graphics interfaces [55, 56];
   - intermediate dumps of the key distributions with a frequency defined by the user;
   - machine independent universal random number generator [57];
   - the complete double precision version 13.1(95) and the version 13.2(95) with all crucial computations in double precision mode are currently supported on SunOS, SGI-IRIX, IBM-AIX and HP-UX; with certain limitations the version 13.2(95) is available for VMS and MS-DOS.

Initial particle kinetic energy is from threshold to 30 TeV. Threshold kinetic energies are 0.00215 eV for neutrons, 0.2 MeV for electrons and photons (0.01 Mev optional), and 2 MeV for all other particles. Transported particle types and their codes (*jj*) are given in Table 1. All other particle types generated at the event processing stage are converted at the production point into the states listed in the table: π^0-mesons are decayed into two photons; ρ-, ω-, D-, and J/Ψ- particles are decayed into muons etc. Heavy fragments (d, t, α and others) deposit their energy locally.

Table 1 : Transported particle types.

jj=	1	2	3	4	5	6	7	8	9	10	11	12
	p	n	π^+	π^-	K^+	K^-	μ^+	μ^-	γ	e^-	e^+	$\tilde{p}$

2.3 Structure

The MARS code system consists of a few hundred FORTRAN77 subroutines accompained (for convenience) by the CERN FFREAD package to read format-free data cards, and by a few CERN service *C*-routines. The system is linked to the CERN library to use the HBOOK package [55]. The output files are analysed with the PAW system [56] and with other graphics packages (TOPDRAWER, GNUPLOT, XMGR and KALEIDAGRAPH). The source code file structure is listed in Table 2.

After compilation with a `-r8` option, version 13.1(95), or without this option for version 13.2(95), all object files are combined into the library **m13lib.a**. File **m13.f** is present in the working directory to allow problem-dependent modifications if needed. File **m13hist.f** can be kept in the same directory. The main input file MARS.INP must be present in the directory. A few other files should be present if a corresponding option is active: GEOM.INP for extended geometry description; link to `dat` directory with `.ndt` files with low-energy neutron cross-sections; files generated with DTUJET and STRUCT (if any). The main output file MARS.OUT along with files to interface with PAW and other graphics systems, and a few additional files for a multi-stage mode, will be created in the directory. All the I/O file names can easily be re-defined by the user in the main program.

An example of the MAIN program with HBOOK and random number generator initializations, with statements to open the main input and output files as well as files to communicate with graphics packages, is presented in the following section.

Table 2 : Source code structure.

File name	Content
m13.f	main program and user routines;
m13bldt.f	all the BLOCK DATA modules;
m13cstuff.c	a few *C* service routines from the CERN library;
m13hist.f	histogram set up and entry subroutines;
m13io.f	I/O and initialisation subroutines;
m13mareg.f	event processing and geometry module;
m13ph.f	all the physics simulation subroutines;
m13tr.f	all the particle transport subroutines;
m13util.f	utility subroutines, including FFREAD.

2.4 MAIN Example

```
IMPLICIT REAL (A-H,O-Z), INTEGER (I-N)
LOGICAL IND
COMMON/LOGIND/IND(20)
COMMON/INPOUT/NREAD,NWR,NWPSI,NWMJL,NWEGH
PARAMETER (LUNHIST=40)
PARAMETER (NH=2500000)
COMMON/PAWC/H(NH)
CHARACTER*20 HISTFILE
CALL HLIMIT(NH)
HISTFILE='MARS.HIST'
CALL HROPEN (LUNHIST,'HBOOK',HISTFILE,'N',1024,ISTAT)
CALL RNDMST(12,34,56,78)
CALL RNDMTE(0)
NREAD=15
NWR= 16
OPEN (UNIT=NREAD,FILE='MARS.INP',STATUS='OLD')
OPEN (UNIT=NWR, FILE='MARS.OUT',STATUS='UNKNOWN')
CALL BEGINN
IF(IND(18)) THEN
OPEN (UNIT=11,FILE='GEOM.INP',STATUS='OLD')
CALL GREAD
END IF
CALL MHISET
NWEGH=17
OPEN(UNIT=NWEGH,FILE='MUON.EGH' ,STATUS='UNKNOWN')
OPEN(UNIT=20, FILE='MUON.PLOT',STATUS='UNKNOWN')
CALL MARSON
NWPSI=13
OPEN(UNIT=NWPSI,FILE='PSINEU.GRA',STATUS='UNKNOWN')
NWMJL=12
OPEN(UNIT=NWMJL,FILE='EDMJL.GRA',STATUS='UNKNOWN')
CALL SERVN
IF(IND(13)) CALL MARACT
CALL HCDIR ('//HBOOK',' ')
CALL HROUT (0,ICYCLE, ' ')
CALL HREND ('HBOOK')
END
```

2.5 Usage

First, MARS.INP and other input files are created by the user. Then, if needed, he/she deals with user subroutines in a file **m13.f** re-defining any of the default parameters and adding a variety of the features to the considered problem (see Chapter 4). If low-energy neutron transport is to be considered with option `IND(14)=T`, the code will look for a directory `ntdir`. The following soft link should be created `ln -s ~/mars13/dat ndtdir`. The command files for compiling and linking MARS under different operating systems are given in Table 3 for version 13.1(95) in global double precision mode. If one uses version 13.2(95) with only all crucial computations in double precision mode, then `-r8` option must be omitted. An executable file called **rma** will be created. For MARS code availability, comments and other related contact `mokhov@fnalv.fnal.gov`.

Table 3 : Command files for version 13.1(95). The option `-r8` (`-qdpc` on IBM-AIX and `-R8` on HP-UX) must be omitted for version 13.2(95).

System	Command file
SunOS	`f77 -o rma -r8 m13lib.a m13.f $ cernlib`
SGI-IRIX	`f77 -o rma -r8 -mips2 m13lib.a m13.f $ cernlib`
IBM-AIX	`f77 -o rma -qdpc -qextname m13lib.a m13.f $ cernlib`
HP-UX	`f77 -o rma -R8 -K +ppu m13lib.a m13.f $ cernlib`

3 General Input

3.1 Framework

There are three levels of the input data definition in MARS: defaults, input cards and user subroutines. All input data have some default values (see next two sections), so if these are acceptable for particular run their presence in the input sequence is not necessary. The shortest input consists of two cards in MARS.INP: a title and the STOP card.

Default values are built into the code. Input cards are defined by the user in two files: MARS.INP (main input sequence) and GEOM.INP (presented and used for the extended geometry description, if `IND(18)=T`). The names of these two files are defined in the main program (file **m13.f**) and can be changed. The main program also allocates the dynamic memory for HBOOK and gives control to the whole system. Histogram set up and entry routines, defined in the file **m13hist.f**,

can be re-defined by the user according to his/her specific needs. All the user subroutines are collected in the **m13.f** file in the dummy form, i. e. a subroutine name followed by the RETURN and END statements. Corresponding subroutines can be modified by the user if necessary.

The user can re-define any of the default parameters with the card input sequence in the file MARS.INP. This consists of option and data cards which allow easy definition of beam parameters, materials, energy thresholds, termination conditions, hA-vertices parameters, geometry and scoring parameters. Multi-medium 3-D cylindrically symetric (r-z-ϕ) "*standard*" geometries and sources can be defined at this stage in a user-friendly fashion. The "*extended*" geometry option extends this friendly way to a combination of boxes, cylinders, spheres and cones, defined in the input file GEOM.INP. In the case of complex composite materials, of very complex geometries, of arbitrary sources and magnetic fields appropriate user subroutines should be provided (see Chapter 4). Arbitrarily complex geometry is usually built into "*standard*" or "*extended*" geometry.

The MARS.INP file consists of a title card in a A80-format followed by some data cards. The standard CERN FFREAD package is used to read these format-free data cards in the routine BEGINN. The structure of all these cards is the same:

KEYW a1 a2 ... N1= b1 b2 ... N2= c1 c2 ...,

where **KEYW** is a keyword assigned to the group of FORTRAN variables a(i), b(i) and c(i); N1 and N2 are the addresses of the arrays b(i) and c(i). The variables may be of the following types: integer, real and logical (represented by T or F). Items are separated by blanks. The order of the the data cards and their number are arbitrary. The only requirement is: the STOP card must be included and must be the last in the sequence. The card image input sequence is described in detail in the following section and cumulatively in Table 6 of Section 3.4. Examples of the input sequence are given in Section 3.5.

The units in MARS are: energy in GeV, dimensions in cm, azimuthal angle ϕ in *degrees*, temperature rise ΔT in degrees Centigrade. The reference system is *global* Cartesian coordinate system (GCS). Typically the origin $x = y = z = 0$ coincides with the source starting point. Any number of *local* coordinate systems (LCS) can be placed in it via GEOM.INP and/or user routines REG1, REG2, ALIGN and SAGIT. In the global system the z is longitudinal, and the positive direction is from left to right. The z axis is usually the center of symmetry, and as a rule the beam strikes along this axis in the positive direction. The positive direction of the x axis of the global system is up and the y axis is toward the viewer, completing a right-handed system.

3.2 Card Input Sequence (MARS.INP)

The first card is a variable MTEXT (FORMAT(A80)) – title of the problem, prints out a heading for the output.

Then some number of unformatted data cards follows.

INDX IND(20)

Logical variables which control the options. Default: 20*F.

IND(1)=T – the program calculates and prints distributions of e^+e^- and photon fluxes and of energy deposition density ϵ and related values: dose equivalent, instantaneous temperature rise ΔT at given initial temperature T_0=TEMPO and number of particles per beam N_0=AINT (see VARS), and contact dose due to induced radioactivity at N_0 beam intensity. Other values discussed in Section 5.1 are calculated independently of the IND(1) meaning.

IND(1)=F – does not calculate the energy deposition related values and reduces execution time drastically in the TeV energy region.

IND(2)=T – initiates "Z – *sandwich standard*" geometry as a basis (see ZSEC and RSEC).

IND(2)=F – initiates "R – *sandwich standard*" geometry as a basis (see ZSEC and RSEC).

IND(3)=T – initiates calling of user subroutines described in Chapter 4 and defined in a file **m13.f**.

IND(3)=F – no user subroutines calling.

IND(4)=T – indicates the presence of magnetic or electric fields in the system; field components must be defined in a user subroutine FIELD.

IND(4)=F – no magnetic or electric fields.

IND(5)=T – activates e^+, e^-, γ and h production by muons at IND(10)=T and knock-on electron and e^+e^--pair production by hadrons;

IND(5)=F – above production mechanisms are not activated.

IND(6)=T – provides the use of mathematical expectation method: scoring of probabilities for a fluence calculation rather than direct (analog) particle contributions; can be effective for "deep penetration" problem (thick shields etc.); use with care, test first.

IND(6)=F – "analog" scoring of transported particles.

IND(7)=T – indicates that an incident particle interacts with probability EFF (see VARS) with the point-like target placed in the system at coordinates (x_0, y_0, z_0) and starts with probability (1−EFF) from this point interacting with the rest of the system. By convention the material index for this target is equal to IM=1, and can be easily re-defined in a BEG1 user subroutine.

IND(7)=F – no point-like target.

IND(8)=T – provides the maximum amount of output to be printed.

IND(8)=F – corresponds to standard output (see Section 5.1).

IND(9)=T – provides the use of special algorithm (as in [22, 42]) for construction of particle trajectories prior to the first two inelastic nuclear interactions (edge scattering problem) and of Landau fluctuations simulation.

IND(9)=F – does not use the above sophisticated algorithms (time saving).

IND(10)=T – activates forced muon production in long and short lived meson decays as well as produced and incident muon transport with all possible interaction processes included (see Section 2.2).

IND(10)=F – turns off muon option (much faster).

IND(11)=T – provides an azimuthal structure of scoring; adds the ϕ– dimension to the *standard* (*r*-*z*) geometries.

IND(11)=F – no azimuthal division option.

IND(12)=T – activates biased antiproton production at every hA-vertex above threshold with a consequent transport.

IND(12)=F – no forced antiproton production.

IND(13)=T – provides specific activity and residual dose rate calculation.

IND(13)=F – no induced radioactivation calculation.

IND(14)=T – provides multi-group neutron transport in the 0.00215 eV to 14.5 MeV energy range using the default 28-group neutron cross-section library; includes photoneutron production at IND(1)=T.

IND(14)=F – turns off low-energy transport; their contribution into energy deposition distribution is considered in a simplified way (much faster).

IND(15)=T – variance reduction via low-energy neutron splitting.

IND(15)=F – no splitting for neutrons.

IND(16)=T – variance reduction via low-energy neutron delta-scattering and weight window at IND(14)=T.

IND(16)=F – no delta-scattering and weight window for neutrons.

IND(17)=T – initiates using of the 49-group cross-section library for neutron transport below 18 MeV and photon production and transport in the 0.01 to 11 MeV energy range produced by these neutrons at IND(14)=T.

IND(17)=F – uses default 28-group neutron cross-section library with no low-energy photon treatment.

IND(18)=T – initiates using of the *extended* geometry algorithm with a reading of an input file GEOM.INP (see Section 3.3).

IND(18)=F – no *extended* geometry description and a file GEOM.INP presented.

IND(19) and IND(20) are not used in the current version.

NEVT NSTOP, NTIME

NSTOP– number of events (or incident particles) to be run. Default: 200.
NTIME– number of intermediate dumps of key results, defined in a user subroutine DUMP. Default: 0.

ENRG E0, EM, PSTAM, EMI, EMNU

E0– incident particle kinetic energy. Default: 100.
EM– hadron energy cutoff for flux and spectra scoring. Default: 0.0145.
PSTAM– star production threshold momentum. Default: 0.3 GeV/c (corresponds to 47 MeV for nucleons and 191 MeV for pions).
EMI– muon energy cutoff for flux and spectra scoring. Default: 0.005.
EMNU– neutrino energy cutoff. Default: 0.5.

IPIB I0, IBEAM

I0– incident particle type (see Table 1). Default: 1.
IBEAM– type of the incident beam, represents the beam profile:
0 – laterally infinitesimal beam;
1 – beam is distributed uniformly in the rectangular area with SIXX and SIYY half-sizes (along the corresponding axis);
2 – beam is Gaussian with R.M.S. equal to σ_x=SIXX and σ_y=SIYY;
3 – beam is Gaussian as defined for IBEAM=2 and additionally has a Gaussian angular spread with R.M.S. equal to $\sigma(\theta_x)$=SITX and $\sigma(\theta_y)$=SITY in radians. Default: 0.

BEAM SIXX, SIYY, SITX, SITY

SIXX, SIYY, SITX, SITY– defined above, active if IBEAM$\geq$1. Default: 0 0 0 0.

INIT XINI, YINI, ZINI, DXIN, DYIN, DZIN

XINI, YINI, ZINI– are initial x_0, y_0, z_0 coordinates of the beam spot center. Default: 0 0 0.

DXIN, DYIN, DZIN– are initial direction cosines of the beam. Default: 0 0 1.

The user can provide his own arbitrary source in a subroutine BEG1 (See Section 4.2).

SMIN STEPEM, STEPH

STEPEM– is an accuracy (in cm) of boundary localization in the iterative transport algorithm, this is a second (in addition to NSTOP) control parameter for calculational accuracy. Recomendation: STEPEM $\simeq 0.3 \times t_{min}$, where t_{min} is a smallest dimension of the smallest cell in the considered system. The larger STEPEM, the faster calculations. Default: 0.3.

STEPH– is a parameter which modestly controls calculational time per event ($\simeq \log(STEPH/STEPEM)$) and accuracy of construction of particle trajectories up to the first two inelastic nuclear interactions for the default case IND(9)=F. Recomendation: STEPH=min(λ, l) where λ is the mean inelastic length for hadrons and l is the length of the characteristic zone in the direction of predominant propagation of the particles. Default: 10.

VARS EFF, DLEXP, TEMPO, AINT

EFF– point-like target efficiency; active if IND(7)=T. Default: 0.

DLEXP– is an exponential conversion factor, which allows for increasing (DLEXP $\geq$1) or decreasing (DLEXP $\leq$1) the effective inelastic mean free path; usefull correspondingly for "deep penetration" problem and for compact restricted systems. Recomendation: 0.3$\leq$DLEXP$\leq$3. Default: 1.

TEMPO– is an initial temperature T_0 in $Kelvin$, defined in the region $4 \leq T_0 \leq 1800$. Default: 300.

AINT– is a number of particles per beam N_0; necessary for calculations of a temperature rise (N_0 is assumed to be for a single instantaneous spill) and crude estimation of a contact residiual dose (here N_0 is assumed to be an average beam intensity in *protons per second*). Default: 10^{12}.

NMAT NREMA

NREMA– is a number of different materials to be included in the particular run. Materials can be single elements (built-in or defined by the user) or complex compounds. The subroutine BEGINN calculates the effective atomic masses and numbers, cross-sections, radiation lengthes and some other quantities. 1≤NREMA≤20. Default: 1.

MATR AMA(20), ROW(20), ATW(20), ZAW(20)

This determines the NREMA specific materials. Special index IM=i is assigned to each material according to the input order. By definition IM=0 corresponds to *vacuum* and IM=NREMA+1 to outside of the global volume (*blackhole*) and the user does not need to include them in the MATR sequence. There are 22 other built in materials: H, LHE, LI, BE, CH2, CH, C, TISS, WATR, AIR,SOIL, CONC, AL, SI, LAR, TI, FE, CU, W, PB, U, BLA1 (see Table 5, Section 3.4). If AMA(i) coincides with one of these names, one does not need to define ROW(i), ATW(i), ZAW(i) for this i. If not, the user must define the material with its corresponding parameters as follows:

i) for single elements – arbitrary name AMA(i), density ROW(i) in g/cm^3, atomic mass ATW(i) and atomic number ZAW(i).

ii) for each composite material – put in the MATR sequence the word 'MIXT' and density ROW(i) and provide the corresponding definition of its composition in a subroutine MIXTUR (see Section 4.1), according to the input order. Default: FE.

NLNG LZ, NLZ

LZ– is a number of longitudinal sections in the system for the *standard* geometry sector. 1≤LZ≤50. Default: 1.

NLZ– multiplicates number of sections, described by ZSEC, i. e. repeats these sections NLZ times; active only for NLZ≥2. Default: 1.

ZSEC ZSE(50), IZN(50), IZI(50), IZM(50)

ZSE(i) – z-coordinate of the right boundary of i-section.
Default: 100., 49*0.

IZN(i) – number of subsections in i-section. Default: 50*1.

IZI(i) – material index IM of i-section, active for IND(2)=T.
Default: 50*1.

IZM(i) – magnetic field index MA of i-section, active for IND(2)=T and IND(4)=T. Default: 50*0.

Maximum total number of the longitudinal subdivisions in the *standard* sector of the current MARS version is MZ=250 and can be easily increased in the *extended* sector and/or in a user subroutine REG1. In the program by definition the smallest z-coordinate is ZMIN, most often ZMIN=z_0=0. The maximum longitudinal dimension of the system is ZMAX – the largest z-coordinate.

NLTR LR

LR is a number of radial sections in the system for the *standard* geometry sector. In the current version LR $\leq$ 20. Default: 1.

RSEC RSE(20), IRN(20), IRI(20), IRM(20)

RSE(i) – radius of i- lateral section. Default: 5.,19*0.

IRN(i) – number of radial subsections in i- lateral section. Default: 20*1.

IRI(i) – material index IM of i- lateral section, active for IND(2)=F. Default: 20*1.

IRM(i) – magnetic field index MA of i- lateral section, active for IND(2)=F and IND(4)=T. Default: 20*0.

Maximum total number of the radial subdivisions in the *standard* sector of the current MARS version is MR=20 and can be easily increased in the *extended* sector and/or in a user subroutine REG1. For IND(11)=F the overall restriction in the *standard* geometry sector is MZ$\times$MR$\leq$5000. Total maximum number of regions is 10000. The maximum radial dimension of the system is RMAX.

NAZM NF

NF is a number of azimuthal bins, 1$\leq$NF$\leq$60. To be presented in the input sequence only if IND(11)=T. Default: 1.

For IND(11)=T the overall restriction for the *standard* geometry sector is NFZP=MZ$\times$MR$\times$NF$\leq$10000. Total maximum number of regions is 10000.

AZIM FIB(60)

The azimuthal grid, 0$\leq$FIB(i)$\leq$360. To be presented in the input sequence only if IND(11)=T and NF$\geq$2. Default: 60*0.

NOBL NOB

NOB is a number of special regions in which particle energy spectra and other histograms will be scored, 0$\leq$NOB$\leq$3. Default: 0.

RZOB RZO(4,3)

Presented in the input sequence only if NOB$\geq$1. Determines the sizes of i-region for particle energy spectra and other histogram scoring:
RZO(1,i) – minimum radius RMI(i), 0$\leq$RMI$\leq$RMAX.
Default: 0.
RZO(2,i) – maximum radius RMA(i), RMI$\leq$RMA$\leq$RMAX.
Default: 0.
RZO(3,i) – left z-coordinate ZMI(i), ZMIN$\leq$ZMI$\leq$ZMAX.
Default: 0.
RZO(4,i) – right z-coordinate ZMA(i), ZMI$\leq$ZMA$\leq$ZMAX.
Default: 0.

PLOT RPLOT, ZPLO1, ZPLO2, ZPLO3

Control a simple plotting of the geometry cross-sections.
RPLOT– maximum x or y coordinate to be presented in plots;
ZPLO1– z-coordinate for the first cross-section of geometry;
ZPLO2– z-coordinate for the second cross-section of geometry;
ZPLO3– maximum z-coordinate of geometry to be printed.
If all these numbers are equal to zero there is no plotting.
Default: 0 0 0 0.

NEUS NG, NGOUT, NINT, NGMAX(20)

NG– number of neutron energy groups in the BNAB/MARS cross-section library. Default: 28.
NGOUT– cutoff group number (see Tables 7 and 8 below). Default: 26.
NINT– number of intervals in the angular flux presentation. Default: 20.
NGMAX(i) – cutoff group number with group-to-group transfers for a material with IM=i. Default: 20*11.
This card can be presented at IND(14)=T.

NDET NDE1

NDE1– number of point-like detectors for energy spectrum, flux and energy deposition of low-energy neutrons at IND(14)=T. 0$\leq$NDE1$\leq$10.
Default: 0.

FLOC RD, XD(10), YD(10), ZD(10)

RD– radius of the point-like detectors for low-energy neutrons. Default: 0.5.
XD(i), YD(i), ZD(i) – coordinates of i-detector. Default: 30*0.
This card is presented at IND(14)=T and NDE1$\geq$1.

NCHO NTYZ(6)

NTYZ(i) – parameters of the systematic selection for low-energy neutrons at IND(14)=T. Default: 2, 2, 1, 3*0.

FLCH FL(200)

FL(i) – importance function for low-energy neutrons at IND(14)=T. Default: 200*0.

MUON KPHA, IDNDX

KPHA– number of hadron generations to follow, i.e. number of levels in hA vertex tree. Default: 30.

IDNDX– activates muon angular distribution scoring in the NOB special regions at IND(10)=T, if IDNDX=1. Default: 0.

STOP Stops the input session

Any cards given after this are meaningless.

A few examples of the input sequence are presented in Section 3.5.

3.3 Extended Geometry (GEOM.INP)

As indicated above, IND(18)=T extends a user-friendly r-z-ϕ geometry description in a file MARS.INP to a combination of boxes, cylinders, spheres and cones, placed into the global coordinate system (GCS). The code reads via the GREAD routine volume data defined in their own local coordinate systems (LCS) in the input file GEOM.INP. Data in the file are *unformatted*, separated by blanks. In the version 13(95) of MARS the maximum number of volumes defined in this file is equal to NVMAX=1000.

First line of the GEOM.INP file contains NVOLUM and NEXGM. Here NVOLUM is total number of the volumes in the *extended* geometry sector, and NEXGM is NFZP (total number of regions in the *standard* geometry sector), or some bigger number to start a volume numbering in the GEOM.INP file with NEXGM+1. Limitations: 1≤NVOLUM≤NVMAX=1000, NFZP≤NEXGM≤(10000−NVOLUM).

Next NVOLUM lines in the input file describe in an arbitrary order each volume:

```
NV, NT, IM, MA, XR, YR, ZR, C1, C2, ...,
```

where NV is volume sequential number in the *extended* geometry sector; NEXGM≤NV≤NEXGM+1000;
NT – volume type; 1≤NT≤4;
IM – material number (index) of given volume; 0≤IM≤20;
MA – magnetic field index; 0≤MA;
XR, YR, ZR – coordinates of a reference point (RP) of the LCS for given volume;
C1, C2, ... – parameters of given volume.

By convention, the first volume in the above list with NV=NEXGM+1 is the global volume defined in MARS.INP. It contains all other volumes in *standard*, *extended* and user-supplied (REG1) geometry sectors. Usually, this is a "big" cylinder (most often with IM=0). A current set of the volume types and description parameters are given in Table 4.

Table 4 : Current set of volume types in GEOM.INP.

NT	Name	Description
1	BOX	C1 and C2– half-sizes along x and y axes, C3– box length along z axis; RP– center of the lowest z plane; x and y LCS axes are parallel to two perpendicular edges of the lowest z plane; z axis points from center of the lowest z plane to center of the highest z plane; x, y, z axes of the LCS are parallel to those of the GCS.
2	CYLINDER	C1 and C2– inner and outer radii of the cylinder; C3– cylinder length along z axis; RP– center of the lowest z plane; z axis points from center of the lowest z plane to center of the highest z plane; z axis of the LCS is parallel to that of the GCS; x and y axes of the LCS orientation is arbitrarily.
3	SPHERE	C1 and C2– inner and outer radii of the sphere; RP– sphere center; LCS axes oriented arbitrarily.
4	CONE	C1 and C2– inner and outer radii at the lowest z; C3 and C4– inner and outer radii at the highest z; C5– cone length along z axis; RP– center of the lowest z plane; z axis points from center of the lowest z plane to center of the highest z plane; z axis of the LCS is parallel to that of the GCS; x and y axes of the LCS orientation is arbitrarily.

3.4 Materials, Defaults and Energy Groups

For user convenience this section includes information on the MARS built-in materials, on the default parameters and on the low-energy groups in two representations.

Table 5 : Built-in materials. Material number (index) `IM` is assigned to each material according to the input order in the file MARS.INP. By definition `IM=0` corresponds to *vacuum* and `IM=NREMA+1` to the *blackhole* outside the global volume.

NAME	$\rho(g/cm^3)$	A	Z	Material
H	0.071	1.00	1.	Hydrogen
LHE	0.125	4.00	2.	Liq. Helium
LI	0.534	6.94	3.	Lithium
BE	1.85	9.01	4.	Beryllium
CH2	0.94	8.96	4.62	Polyethylene
CH	1.03	10.24	5.2	Polystyrene
C	2.265	12.01	6.	Graphite
TISS	0.99	12.37	6.3	Tissue
WATR	1.00	12.41	6.32	Water
AIR	0.00121	13.05	6.53	Air
SOIL	1.90	20.80	10.40	Soil
CONC	2.35	20.88	10.44	Concrete
AL	2.70	26.98	13.	Aluminium
SI	2.33	28.09	14.	Silicon
LAR	1.40	39.95	18.	Liq. Argon
TI	4.54	47.88	22.	Titanium
FE	7.86	55.85	26.	Iron
CU	8.92	63.55	29.	Copper
W	19.30	183.85	74.	Tungsten
PB	11.35	207.19	82.	Lead
U	18.95	238.03	92.	Uranium
BLA1	10000.	240.00	94.	Black Hole

Table 6 : Optional input variables in MARS.INP and their defaults.

Keyword	Variables and Arrays	Default
	MTEXT	Format(A80)
INDX	IND(20)	20*F
NEVT	NSTOP, NTIME	200, 0
ENRG	E0,EM,PSTAM,EMI,EMNU	100.,.0145,.3,.005,.5
IPIB	I0, IBEAM	1, 0
BEAM	SIXX, SIYY, SITX, SITY	4*0.
INIT	XINI,YINI,ZINI,DXIN,DYIN,DZIN	5*0., 1.
SMIN	STEPEM, STEPH	0.3, 10.
VARS	EFF, DLEXP, TEMPO, AINT	0.,1.,300.,10^{12}
NMAT	NREMA	1
MATR	AMA(20),ROW(20),ATW(20),ZAW(20)	FE, 79*0
NLNG	LZ, NLZ	1, 1
ZSEC	ZSE(50),IZN(50),IZI(50),IZM(50)	100.,49*0.,100*1,50*0
NLTR	LR	1
RSEC	RSE(20),IRN(20),IRI(20),IRM(20)	5., 19*0., 40*1, 20*0
NAZM	NF	1
AZIM	FIB(60)	60*0.
NOBL	NOB	0
RZOB	RZO(4,3)	12*0.
PLOT	RPLOT, ZPLO1, ZPLO2, ZPLO3	4*0.
NEUS	NG, NGOUT, NINT, NGMAX(20)	28, 26, 20, 20*11
NDET	NDE1	0
FLOC	RD, XD(10), YD(10), ZD(10)	0.5, 30*0.
NCHO	NTYZ(6)	2, 2, 1, 3*0
FLCH	FL(200)	200*0.
MUON	KPHA, IDNDX	30, 0
STOP		

Table 7 : Neutron energy group numbers NG and lower energy boundaries EG (MeV) in the group at $E \leq 14.5$ MeV in the 28-group representation. Used with IND(14)=T and IND(17)=F.

NG=	1	2	3	4	5	6	7
EG=	14.	10.5	6.5	4.0	2.5	1.4	0.8
NG=	8	9	10	11	12	13	14
EG=	0.4	0.2	0.1	4.65E-2	2.15E-2	1.E-2	4.65E-3
NG=	15	16	17	18	19	20	21
EG=	2.15E-3	1.E-3	4.65E-4	2.15E-4	1.E-4	4.65E-5	2.15E-5
NG=	22	23	24	25	26	27	28
EG=	1.E-5	4.65E-6	2.15E-6	1.E-6	4.65E-7	2.15E-7	2.15E-9

Table 8 : Neutron energy group numbers NG and lower energy boundaries EG (MeV) in the group at $E \leq 18$ MeV in the 49-group representation.
Used with IND(14)=T and IND(17)=T.

NG=	1	2	3	4	5	6	7
EG=	16.90	15.80	14.80	14.00	13.03	12.12	11.28
NG=	8	9	10	11	12	13	14
EG=	10.50	9.312	8.260	7.327	6.500	5.757	5.099
NG=	15	16	17	18	19	20	21
EG=	4.516	4.000	3.640	3.320	2.881	2.500	2.162
NG=	22	23	24	25	26	27	28
EG=	1.870	1.618	1.400	1.210	1.058	0.920	0.800
NG=	29	30	31	32	33	34	35
EG=	0.400	0.200	0.100	4.65E-2	2.15E-2	1.00E-2	4.65E-3
NG=	36	37	38	39	40	41	42
EG=	2.15E-3	1.00E-3	4.65E-4	2.15E-4	1.00E-4	4.65E-5	2.15E-5
NG=	43	44	45	46	47	48	49
EG=	1.00E-5	4.65E-6	2.15E-6	1.00E-6	4.65E-7	2.15E-7	2.53E-8

Table 9 : Photon energy group numbers NG and lower energy boundaries EG (MeV) in the group at $E \leq 11$ MeV. Used with IND(14)=T and IND(17)=T.

NG=	1	2	3	4	5	6	7	8
EG=	11.	9.	7.	5.5	4.5	3.5	2.5	1.75
NG=	9	10	11	12	13	14	15	
EG=	1.25	0.75	0.35	0.15	0.08	0.04	0.02	0.01

3.5 Input Examples

Example 1. Calculate antiproton production with 9-cm long 1-cm diameter copper target irradiated with 120-GeV proton beam. Beam R.M.S spot size is σ_x=0.005 cm and σ_y=0.007 cm. In addition to forced antiproton production the user is interested in energy deposition calculation including knock-on electron and e^+e^--pair production by hadrons. To create a file of antiprotons generated on the target in a given phase space, the user adds in MAIN:

```
OPEN (UNIT=9,FILE='PBAR.OUT',STATUS='UNKNOWN')
```

and a few statements in the LEAK routine (see Sect. 4.5). The geometry and scoring is described in the *standard* mode. The MARS.INP file can look as:

```
Pbar Cu Target, sigx=0.005, 02-Nov-1994
INDX T 5=T 12=T
NEVT 100000
ENRG 120.
IPIB 1 2
BEAM 0.005 0.007
SMIN 0.001 3.
MATR 'CU'
ZSEC 9.  51=3
NLTR 5
RSEC 0.002 0.005 0.01 0.1 .5
STOP
```

The geometry is very simple here, completely adequate to the *standard* mode. Instead of the above bining and writing to a file PBAR.OUT, one can use HBOOK (see MAIN) for analyses of energy deposition and generated antiprotons. Then the solid target can be described just as:

```
ZSEC 9.
RSEC 0.5
```

Example 2. Intense 800-GeV proton beam hits a graphite dump followed by aluminum and steel absorbers, by 210-cm vacuum gap, by 5-cm polyethylene slab, and finally by 1 meter of a wet dirt. The user is interested in energy deposition calculations, in maximum amount of the output, including partial distributions, temperature rise and estimation of a residual dose rate, in intermediate result dumps. A compound material is defined in the MIXTUR routine (Sect. 4.1). The routines

REG1 and REG2 (Sect. 4.3) define the dump as surrounded with a steel shield sitting at the axis of a hypothetical cylindrically symmetrical tunnel with 30-cm thick concrete walls. With these three user routines a *standard* MARS.INP file can look as (*Option 1*):

```
Tevatron C0 Dump, 02/28/95
INDX T T 8=T
NEVT 500000 5
IPIB 1 2
ENRG 800.
SMIN 0.01 8.
BEAM 0.0416 0.0944
VARS 0.  1.  300.  4.E13
NMAT 6
MATR 'C' 'AL' 'FE' 'CONC' 'CH2' 'MIXT'
26=2.1
NLNG 7
ZSEC 350.  425.  475.  490.  700.  705.  805.
51=14 5 10 1 3 2 5 101=1 2 3 2 0 4 5
NLTR 9
RSEC 0.03 0.1 0.3 1.  3.5 10.  30.  150.  180.
PLOT 5.  300.  450.  805.
STOP
```

Option 2. The geometry description is simpler and the output is more sophisticated if one uses HBOOK activated in MAIN. The last lines in MARS.INP can be re-written as:

```
NLNG 7
ZSEC 350.  425.  475.  490.  700.  705.  805.
101=1 2 3 2 0 4 0 5
NLTR 4
RSEC 10.  30.  150.  180.
```

Option 3. It is worthwhile to use *extended* geometry description in this example. The following changes have to be done to the MARS.INP file:

```
INDX T T T 8=T
NLNG 1
ZSEC 805.
NLTR 1
RSEC 180.
```

A GEOM.INP file can look as:

```
12  1
2   2  0  0  0.  0.  0.    0.    180.  805.
3   2  1  0  0.  0.  0.    0.    10.   350.
4   2  2  0  0.  0.  350.  0.    10.   75.
5   2  3  0  0.  0.  425.  0.    10.   50.
6   2  2  0  0.  0.  475.  0.    10.   15.
7   2  0  0  0.  0.  490.  0.    150.  210.
8   2  5  0  0.  0.  700.  0.    150.  5.
9   2  6  0  0.  0.  705.  0.    150.  100.
10  2  3  0  0.  0.  0.    10.   30.   490.
11  2  0  0  0.  0.  0.    30.   150.  490.
12  2  4  0  0.  0.  0.    150.  180.  805.
```

User subroutines REG1 and REG2 are not needed in this case. Detailed histogramming can be done via HBOOK (as in *Option 2*) or by adding a required number of regions into the files MARS.INP or GEOM.INP. Depending on the application an appropriate combination of the *standard* and *extended* volumes, of the *standard* and HBOOK histogrammings etc., can improve the outcome.

4 User Subroutines

All the user subroutines described below are collected in the file **m13.f** and are called if `IND(3)=T`. By default they are the *dummy* and must be the *dummy* until the user changes them for his/her particular application.

4.1 Compounds (MIXTUR)

The user can define any composite material not built into the current version of MARS (see Table 5) with the help of a subroutine `MIXTUR(I,M,A,Z,W)`. For each non-standard material marked in the input sequence with `'MIXT'` this subroutine has to define number of components in the compound `M`, atomic masses `A(M)`, atomic numbers `Z(M)` and relative fractions of components `W(M)` in the compound. Material index `I` is determined according to the input order of material cards **MATR**. An example of the subroutine (used in the second example of Sect. 3.5) for the case when the first five materials are the pre-defined elements (from Table 5 or described on the input card **MATR**), and the sixth is SiO_2 with 5% of water by weight, is presented below:

```
      SUBROUTINE MIXTUR(I,M,A,Z,W)
      IMPLICIT REAL (A-H,O-Z), INTEGER (I-N)
C     INPUT: I-MATERIAL INDEX. OUTPUT:
C     M - NUMBER OF COMPONENTS, 2≤M≤6
C     A, Z - ATOMIC MASSES AND NUMBERS OF COMPONENTS
C     W - RELATIVE FRACTIONS OF COMPONENTS
      DIMENSION A(1),Z(1),W(1)
      IF(I.LT.6) RETURN
      M=3
      A(1)=28.
      A(2)=16.
      A(3)=1.
      Z(1)=14.
      Z(2)=8.
      Z(3)=1.
      S=0.95*(28.+32.)+0.05*18.
      W(1)=0.95*28./S
      W(2)=(0.95*32+0.05*16.)/S
      W(3)=0.05*2./S
      RETURN
      END
```

4.2 Source (BEG1)

A source term of almost any complexity can be described in a user-written subroutine BEG1(JJ,W,E,X,Y,Z,DX,DY,DZ). This is especially useful when the problem should be solved in two (or more) consecutive steps. BEG1 is used for more efficient calculations in the following cases:

- separate event generator (DTUJET, ISAJET etc.);
- very extended source (e.g., beam loss distributions in accelerators, coupling with the STRUCT code);
- geometrically and energetically extended source (e.g., thermal neutron flux studies in the multi-section labyrinths at accelerators);
- any other pre-calculated source;
- tagging of certain regions in the source particle phase-space.

Any part of an external source can be read. Each call to a subroutine BEG1 must provide a new set of initial particle parameters. In this subroutine the user may re-define any or all of 9 parameters in case he/she wants them to be different from the ones defined in the input sequence. The parameters are particle type (JJ), statistical weight of the current event (W with a default W=1), kinetic energy of initial particle (E), initial coordinates (X, Y, Z) and initial direction cosines (DX, DY, DZ). Before each call to a subroutine BEG1 (once per event) all 9 parameters are equal to input ones and any can be changed inside.

For example, to have incident particles distributed uniformly on a 3.3-cm aperture and along a 600-cm region longitudinally, the user should provide the following subroutine:

```
      SUBROUTINE BEG1(JJ,W,E,X,Y,Z,DX,DY,DZ)
      IMPLICIT REAL (A-H,O-Z), INTEGER (I-N)
C     RE-DEFINES EACH OR ANY OF THE 9 PARAMETERS
C     OF INITIAL SOURCE PARTICLES
C     PARTICLE TAGGING IN 'MTAG' SOURCE ZONES OF 'EG'
C     ENERGY INTERVALS FOR 'NTAG' DETECTOR ZONES
C     DEFAULTS: MTAG=0, INTG=1, IETG=4
C
      COMMON/MATINT/IM
      COMMON/TAGG/ET(60,4,6),EG(4),NTAG(6),MTAG,INTG,IETG
      DATA R,PI/3.5,3.1415926/
C
      A=2.*PI*RNDM(-1.)
      X=R*SIN(A)
      Y=R*COS(A)
      Z=600.*RNDM(-1.)
      RETURN
      END
```

4.3 Geometries (REG1, REG2, REG3)

If one wants to study cascades in a very complex geometry not embraced by the above options, user subroutines REG1 and REG2 must be provided. MARS, version 13(95), allows the user to place geometrical objects of almost any complexity inside the pre-defined *standard* (r-z-ϕ) or *extended* geometry. By convention the total number of *standard* regions NFZP must be NFZP$\geq$1. With the help of his/her own subroutines REG1(X,Y,Z,N,NIM) and REG2(N,IM,MAG) the

user can describe arbitrary physical regions numbered from the NMIN≤N≤NMAX interval. Here NMAX=10000; NMIN=NFZP+1 for the *standard* geometry sector and NMIN=NEXGM+NVOLUM for the *extended* geometry sector. Each region can be divided into any number of arbitrary subregions with index NIM with a default value NIM=0. This feature provides the possibility of distinguishing geometrical zones without scoring results there. The user can successfuly substitute this with the HBOOK histogramming (see MAIN and **m13hist.f**).

For each call, a subroutine REG1(X,Y,Z,N,NIM) finds the position of the given point (X,Y,Z) in the system: it determines the corresponding physical region number N (each with its own material index) and, if one wishes, the subregion number NIM. The second subroutine REG2(N,IM,MAG) attributes to a given N (≥NMIN) the material index IM and, if IND(4)=T, the magnetic index MAG. The last parameter can be used in a subroutine FIELD to determine the type of magnetic field (uniform, dipole, quadrupole etc.) in the region N. Default: MAG=0 (no magnetic field in the region).

By convention the region outside of the global volume has a number N=0 and properties of the *black hole*. In some applications it is useful to tag and to score the leakage out of the non-standard regions into the *black holes* labeled with N≤ −1 to use these negative tags in a user routine LEAK. The user must pay a special attention to careful programming of the subroutine REG1, because the geometrical modules consume usually about 80 % of the CPU time, as is typical of cascade Monte Carlo programs.

Simple examples of the subroutines REG1 and REG2 (used in the second example of Section 3.5) are:

```
      SUBROUTINE REG1(X,Y,Z,N,NIM)
      IMPLICIT REAL (A-H,O-Z), INTEGER (I-N)
C     NON-STANDARD GEOMETRY MODULE
C     FINDS THE PLACE OF GIVEN POINT IN THE SYSTEM
C     INPUT: X, Y, Z
C     OUTPUT:
C     N - PHYSICAL REGION NUMBER, NMIN≤N≤NMAX
C     NMIN=NFZP+1 (STANDARD)
C     OR
C     NMIN=NEXGM+NVOLUM (EXTENDED)
C     NMAX=10000
C     N≤-1 DEFINES NUMBERED LEAKAGE OUT OF THE SYSTEM
C     IN NON-STANDARD SECTOR
C     NIM -GEOMETRICAL SUBREGION NUMBER, 0≤NIM
C
C     REVISION: 28-FEB-1995
C
      R=SQRT(X*X+Y*Y)
      IF(R.LT.10.)  RETURN
      M=500
      IF(R.LT.150.)  THEN
      IF(Z.LT.490.)  THEN
C     STEEL SHIELDING:
      N=M+1
C     TUNNEL:
      IF(R.GT.30.)  N=M+2
      END IF
      ELSE
C     CONCRETE SHELL:
      N=M+3
      END IF
      RETURN
      END
```

```
      SUBROUTINE REG2(N,IM,MAG)
      IMPLICIT REAL (A-H,O-Z), INTEGER (I-N)
C     FINDS MATERIAL AND MAGNETIC INDICES
C     INPUT: N - PHYSICAL REGION NUMBER
C     OUTPUT:
C     IM - MATERIAL INDEX
C     MAG - MAGNETIC FIELD INDEX, IF IND(4)=T
C
C     REVISION: 28-FEB-1995
C     IM=1(C),2(AL),3(FE),4(CONC),5(CH2),6(DIRT)
C
      DIMENSION IMUN(3)
      DATA IMUN/1,0,6/
      M=N-500
      IM=IMUN(M)
      RETURN
      END
```

In some cases it is convenient to re-define a few material and/or magnetic indices assigned to the *standard* or *extended* regions at the initilization stage. This can be easily done in a user routine REG3, e.g.:

```
      SUBROUTINE REG3(N,IM,MAG)
      IMPLICIT REAL (A-H,O-Z), INTEGER (I-N)
C     RE-DEFINES IM AND MAG FOR STANDARD SECTOR
      IF(N.EQ.137) IM=14
      IF(N.EQ.2503) IM=2
      RETURN
      END
```

4.4 Magnetic and Electrical Fields (FIELD, SUFI)

To describe the magnetic field components (BX, BY, BZ) in the regions with parameter MAG$\neq$0 the user puts IND(4)=T and provides a subroutine FIELD. The same routine is used to describe an electrical field. One can use a corresponding map or analytical expressions to find the field components in the point (X, Y, Z). Parameter MAG defined in REG2 can speed up the search. It indicates the type of the field in the region. The unit for magnetic field is $Tesla$. A 2-D or 3-D field map is read in a user routine SUFI at the initilization stage and transfered to the routine FIELD via appropriate COMMON block.

An example of the FIELD subroutine is:

```
      SUBROUTINE FIELD(X,Y,Z,BX,BY,BZ,BBB)
      IMPLICIT REAL (A-H,O-Z), INTEGER (I-N)
C     FINDS COMPONENTS OF MAGNETIC FIELD
C     INPUT: MAG -MAGNETIC INDEX AT GIVEN POINT
C     X,Y,Z - POINT'S COORDINATES (OPTIONAL)
C     FIELD MAPS
C     QUADS GRADIENTS IN T/CM
C     G≥0 FOR FOC QUADS, G≤0 FOR DEFOC QUADS
C     OUTPUT: BX,BY,BZ,BBB IN TESLA
C     REVISION: 16-DEC-1994
C
      COMMON/BLINT2/JJ,KK,MAG
      DATA RAQ,BQUA,G1/8.,2.,0.53/
      BX=0.
      BY=0.
      BZ=0.
      IF(Z.LT.622.)  THEN
      BX=5.
      IF(MAG.EQ.2) BX=-5.
      ELSE
      CALL QUAD(X,Y,R,RAQ,G1,BX,BY)
      CALL DIPOLE(X,Y,R,RAQ,BQUA,BX1,BY1)
      BX=BX+BX1
      BY=BY+BY1
      END IF
      RETURN
      END
```

4.5 Leakage (LEAK)

A user subroutine LEAK(N,K,JJ,W,E,X,Y,Z,DX,DY,DZ) handles particles which escape from the system (N=0) or from the $non-standard$ regions tagged with N≤ -1. Parameter K is the tree vertex level (generation number) for the hadronic part of the calculated cascade. If IND(14)=T, then K has the same meaning as the above if given particle was generated in hA vertex at E>0.0145 GeV, otherwise it is forced to be K=−205, if the leaked neutron was produced in sequent interactions below 0.0145 GeV. JJ is particle type from Table 1. If K=−205, the

particle type is neutron by default and JJ is its energy group number from Tables 7 or 8. W is leaked particle statistical weight, E is its kinetic energy, (X, Y, Z) and (DX, DY, DZ) - its coordinates and direction cosines, respectively.

The routine LEAK used in the first example of Sect. 3.5 to collect generated antiprotons in the file PBAR.OUT looks like:

```
      SUBROUTINE LEAK(N,K,JJ,W,E,X,Y,Z,DX,DY,DZ)
      IMPLICIT REAL (A-H,O-Z), INTEGER (I-N)
C     PARTICLE LEAKAGE SPECIAL SCORING
C     IF(K=-205):  JJ=NGROUP, E=0.0005*(EN(JJ)+EN(JJ+1))
C     FOR L.E.NEUTRONS (E≤0.0145 GEV)
C     REVISION: 02-NOV-1994
      COMMON/STAZI1/ZMAX,REXT
      DATA POPT,DP0,DZ0/8.9,0.022,0.99/
C
      IF(JJ.NE.12) RETURN
      IF(DZ.LE.DZ0) RETURN
      P=SQRT(E*(E+1.87656))
      DP=ABS((P-POPT)/POPT)
      IF(DP.GT.DP0) RETURN
      WRITE(9)E,W,X,Y,Z,DX,DY,DZ,K
      RETURN
      END
```

4.6 Fictitious Scattering (ALIGN, SAGIT)

In some applications components of the considered system can be turned or shifted with respect to each other. Say, the arc of any circular accelerator is built of the magnets turned by a fixed angle. MARS, version 13(95), allows an elegant way to handle such systems. The user describes the geometry as the straight along the z-axis. Then, with the help of a routine ALIGN, he/she creates the angular or space kicks at the required boundaries in the directions *opposite* to the real ones. One can easily see that the resulting coordinates and angles of any particle are identical to those in the real *bent* geometry. It is convenient to use spare NIM parameters to control such "a fictitious scattering" at the required boundaries with NIB≠NIM as that parameter in a previous region. Of course, any coordinate can be used to locate the needed boundary.

The following example shows use of the ALIGN routine for a single kick:

```
      SUBROUTINE ALIGN(X,Y,Z,DX,DY,DZ,NIM,NIB)
      IMPLICIT REAL (A-H,O-Z), INTEGER (I-N)
C     FICTITIOUS SCATTERING : DISCRETE AT BOUNDARIES
C     RE-DEFINES EACH OR ANY OF THE FIRST 6 PARAMETERS
C
      DATA ANG/1.5E-3/
      IF(NIB.EQ.1050.AND.NIM.EQ.2010) THEN
      DY=DY-ANG
      END IF
      RETURN
      END
```

The same method is used in MARS to handle objects with saggita, i.e. continuously bent. "Fictitious scattering" defined in a user subroutine SAGIT as an *anti-kick* at every step along charged and neutral particle trajectories, simplifies the geometry description and makes a precise correspondence to the real bent objects.

4.7 Edge Scattering (EDGEUS)

If the "edge scattering problem" is considered with IND(9)=T and the geometry includes *non – standard* insertions defined with REG1 and REG2, the user should supply a subroutine EDGEUS(X,Y,Z,DX,DY,DZ,U,V). It finds the distance U from the given trajectory point (X,Y,Z) to a non-standard surface, and the projection V of the direction vector (DX,DY,DZ) to the normal to the surface which passes in its positive direction through the point (X,Y,Z).

This example shows use of the EDGEUS routine for the surface Y=YPL>0 and for the particle with Y>YPL and DY<0:

```
      SUBROUTINE EDGEUS(X,Y,Z,DX,DY,DZ,U,V)
      IMPLICIT REAL (A-H,O-Z), INTEGER (I-N)
C     EDGE-SCATTERING PROBLEM
      U=Y-YPLANE
      V=DY
      RETURN
      END
```

4.8 Special Volumes (VFAN)

In a *standard* geometry sector the volumes of the regions needed, for example, to compute energy deposition density in GeV/g, are calculated at the final stage in the SERVN subroutine. The array of volumes VV of the $non-standard$ regions M should be provided by the user in a subroutine VFAN(N,V). The same subroutine can be used in specific activity and residual dose rate calculations at IND(13)=T. The VFAN routine can look as:

```
      SUBROUTINE VFAN(N,V)
      IMPLICIT REAL (A-H,O-Z), INTEGER (I-N)
C     FINDS VOLUME V, CM**3 OF REGION N>NFZP
      DIMENSION VV(2)
      DATA VV/1.53E4,7.34E6/
      M=N-750
      V=VV(M)
      RETURN
      END
```

4.9 Intermediate Dumps (DUMP)

A parameter NTIME≥1 in the input sequence of MARS.INP creates dumps of the inermediate results NTIME times. The user defines in the subroutine DUMP(NDUMP) what to display on screen and to store in the file DUMP:

```
      SUBROUTINE DUMP(NDUMP)
      IMPLICIT REAL (A-H,O-Z), INTEGER (I-N)
C     DUMP OUTPUT NTIME≥1 TIMES, NUPRI=NSTOP/NTIME
C     NDUMP - NUMBER OF DUMPED REGIONS
      NWDUMP=14
      OPEN (NWDUMP,FILE='DUMP',STATUS='UNKNOWN')
      CALL DATIMH(MDATE,MTIME)
      WRITE(6)MDATE,MTIME,NI,NSTOP,NUPRI,NDUMP
      WRITE(NWDUMP)MDATE,MTIME,NI,NSTOP,NUPRI,NDUMP
C     WRITE NEEDED RESULTS TO 'DUMP' FILE HERE:
C
      CLOSE (NWDUMP)
      RETURN
      END
```

5 Output

There are three levels of the MARS, version 13(95), output which are essentially self-explainatory:

- general output in the file MARS.OUT;
- a file MARS.HIST defined in MAIN and filled by HBOOK for further analyses with PAW and other tools;
- a few files to be used by graphics packages PAW and others (.GRA, .PLOT) and to be used in a consecutive run in a multi-stage case; the files are defined in the MAIN subroutine (see Sect. 2.4).

5.1 General Output (MARS.OUT)

A file MARS.OUT consists of two major sections: input status and printout of the Monte Carlo session results.

A. Input Status

The subroutine BEGINN prints the cards it has read and some calculated quantities to be used in the Monte Carlo session. Every value is provided with the corresponding keyword and title. The following is printed consecutively: code version number, date and time, title of the problem, options logical statement, requested numbers of incidents (events) and of intermediate dumps, incident particle and beam types, incident kinetic energy, particle fluence cutoff energies, star production threshold, incident particle type, initial coordinates and direction cosines of the beam spot center, R.M.S. beam spot sizes and angular spread, accuracy of boundary localization STEPEM and control parameter STEPH, point-like target efficiency, exponential conversion factor, initial temperature, beam intensity, number of hA generations to follow.

Then for each material the following values that have been either read in or calculated are printed: material index, material name, averaged atomic mass and atomic number, averaged electron density, ionization potential, critical energy and radiation length, contents of composite materials (if any), threshold energies for δ-electrons and direct e^+e^- pair production by charged hadrons, calculated lengths for inelastic hadron-nuclear interactions at incident energy E0 and ionization ranges at the cutoff energy EM.

If IND(14)=T information on low-energy neutrons is printed: content of the **NEUS** card, group cross-sections for each material, number of point-like detectors and their coordinates (if any).

If IND(11)=T there is a printout of the azimuthal grid and if NOB$\geq$1 a printout of radial and longitudinal boundaries of macro-regions for particle spectra scoring.

If all of RPLOT, ZPLO1, ZPLO2, ZPLO3 are not equal to zero, two lateral and one longitudinal cross-sectional views will be drawn.

B. Printout

First, for the *standard* (r, z, ϕ) part of the considered geometry, a table is printed which indicates correspondence of region boundaries and index N, assigned to each region. Also printed are corresponding material and magnetic field indices. The calculational results are referenced to this table by a region number N.

The MARS.OUT file contains the results of the Monte Carlo session as a number of tables and single quantities. All results are normalized to one incident particle (to one event), only temperature rise and residiual dose distributions are normalized to AINT incidents (events). The following tables are printed here consecutively:

1. Longitudinally integrated lateral distributions of charged and total star density and hadron flux, of partial and total energy deposition.

2. Laterally integrated longitudinal distributions of partial and total energy deposition, corresponding cumulative distribution and total energy deposited via the different channels: neutron reactions below EM, low-energy particles from the nuclear de-excitation processes, electromagnetic showers and ionization losses of charged hadrons and muons.

3. Three-dimensional star density distribution *(stars per cubic centimeter)* induced by charged hadrons and by all hadrons for momenta $\geq PSTAM$ with corresponding statistical errors (one R.M.S.). Collision estimator.

4. Three-dimensional total hadron flux distribution *(particles per centimeter squared)* for kinetic energy $\geq$EM with corresponding statistical errors. Track-length estimator.

5. Three-dimensional charged hadron flux distributions for kinetic energy above two thresholds, 0.0145 and 0.5 GeV as a default.

6. Three-dimensional e^+e^- flux distributions for kinetic energy above two thresholds, 0.001 and 0.005 GeV as a default, if `IND(1)=T`.

7. Three-dimensional photon flux distributions for kinetic energy above two thresholds, 0.001 and 0.005 GeV as a default, if `IND(1)=T`.

8. Three-dimensional muon flux distributions for kinetic energy above two thresholds, 0.005 and 0.5 GeV as a default, if `IND(10)=T`.

9. Three-dimensional neutron (E<0.0145 GeV) flux distribution *(particles per centimeter squared)* with corresponding statistical errors, if `IND(14)=T`.

10. Total number of stars produced in the system.

11. Laterally integrated longitudinal distributions of star density, of total hadron flux, and of charged hadron, e^+e^- and muon fluxes.

12. Three-dimensional distribution of energy deposition density brought by low-energy particles from de-excitation of nuclei, in *GeV/g*, if `IND(1)=T`.

13. Three-dimensional distribution of energy deposition density of electromagnetic showers produced by π^0 decays, by high energy $\delta-$rays and by prompt e^+e^- pairs from hadrons, in *GeV/g*, if `IND(1)=T`.

14. Three-dimensional distribution of energy deposition density from hadron and muon electromagnetic losses with limited energy transfer, in *GeV/g*, if `IND(1)=T`.

15. Three-dimensional distribution of energy deposition density due to neutron interactions below E<0.0145 GeV, in *GeV/g*, if `IND(14)=T`.

16. Three-dimensional distribution of total energy deposition density with corresponding statistical errors (one R.M.S.), in *GeV/g*, if `IND(1)=T`.

17. Three-dimensional distribution of dose equivalent, in *Rem*, if `IND(1)=T`.

18. Crude estimation of three-dimensional distribution of residual dose rate, in *Rad/hr*, after 30-day irradiation at the mean beam intensity `AINT` particles per sec and 1-day cooling. These are valid only for sufficiently thick systems, beyond a lateral thickness of $\geq \lambda_{in}$.

19. Three-dimensional distribution of instantaneous temperature rise at given initial temperature T_0=TEMPO and number of particles per a single beam pulse N_0=AINT, if IND(1)=T.

20. Longitudinal distribution of relative energy deposition by charged particles falling below the thresholds. Two distributions presented if IND(1)=T, are for the first smallest radial bin and for the rest of the system.

21. Three-dimensional distribution of the *relative* statistical errors of star densities, fluxes and energy deposition densities.

22. Leakage data: number and energy of albedo hadrons, of punchthrough hadrons and of hadrons that escaped the sides of the system; leakage energy of low-energy neutrons and of electromagnetic showers; total leakage energy; energy balance.

23. Leakage energy spectra of different particles for the upstream plane, downstream plane and for the rest of the system.

24. If NOB$\geq$1, energy spectra of different particles in the pre-determined special regions.

25. Tables of particle spectra, of star density, of hadron, muon and low-energy fluence, of total energy deposition density, and of temperature rise, ready for use with graphics packages. The same tables are saved in separate .GRA files if activated in MAIN.

If IND(8)=F, the tables No. **5–7, 12–14, 17, 18, 20, 21** will be absent in the output.

If IND(18)=T, most of the above values will be printed in a compact form for the *extended* geometry regions as with IND(8)=F.

If the user defines geometrically complex insertions defined with REG1 and REG2 routines as a supplement to the *standard* and *extended* geometries, additionally the program prints in a compact form most of the above quantities with corresponding statistical errors for all $non - standard$ regions.

5.2 Histograms

In many cases it is worthwhile to initialize in the MAIN program the HBOOK package to use the output file MARS.HIST for interactive analysis with the PAW system. Then all the powerful features of that system as described in [56] can be used for comprehensive physics analysis of the run session. By default MARS sorts histograms by following classes:

- histogram type (vertex, fluence, energy deposition and energy spectrum);
- particle class (hadron, electromagnetic and muon);
- charge (neutrals, charged and total).

These histograms are filled for the whole system or for the NOB special regions defined in the MARS.INP file. The histogram list in the file MARS.HIST with their IDs and functional contents is obtained with the PAW command `hi/list`. The list is self-explainatory. Default histogram IDs are shown in Table 10. A few examples of corresponding analyses are given in the next section.

Table 10 : Default histogram ID at `NOB=1`.

Particle	Vertex	Fluence	Energy Dep.	Spectrum
n	1	101		301
$h^{\pm}$	2	102		302
Total h	3	103	203	
γ	4	104		304
$e^{\pm}$	5	105		305
Total EM	6	106	206	
$\mu^{\pm}$	8	108	208	308

6 Physics Analyses: Examples

Results of MARS.OUT can be used as a final product. In addition, the created files .GRA and .PLOT are ready for acceptance by the popular graphics packages PAW, TOPDRAWER, GNUPLOT, XMGR and KALEIDAGRAPH to create high resolution plots for most of the distributions listed in the previous section. Figure 1 is a typical plot obtained via such an interface. The figure shows energy deposition rate in the C-layer of the SAMUS/WAMUS muon spectrometer of the D0 detector at Fermilab for two shielding configurations. Results are obtained with 4000 DTUJET93 events (0.9×0.9 TeV $p\tilde{p}$ collisions).

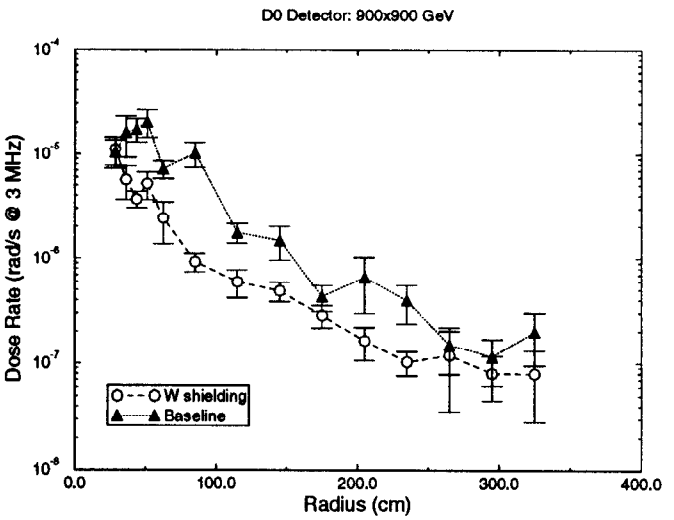

FIGURE 1. Dose rate in the forward muon system of the D0 detector at Fermilab.

Figure 2 (histogram `ID=203`) represents energy deposition density in the forward region of the D0 detector at Fermilab. Interactions of particles, produced in the $p\tilde{p}$ collisions, with detector and accelerator components in this region (4 to 10 meters from the collision point) are the major source of backgrounds in the forward muon spectrometer. All the details of geometry and magnetic field were taken into account in MARS coupled here with DTUJET93. The figure highlights the hottest objects and immediately indicates if the levels in the chamber are above the tolerable one. A similar plot for particle fluxes identifies the channels for radiation to reach critical regions and helps to find an appropriate absorber to plug them.

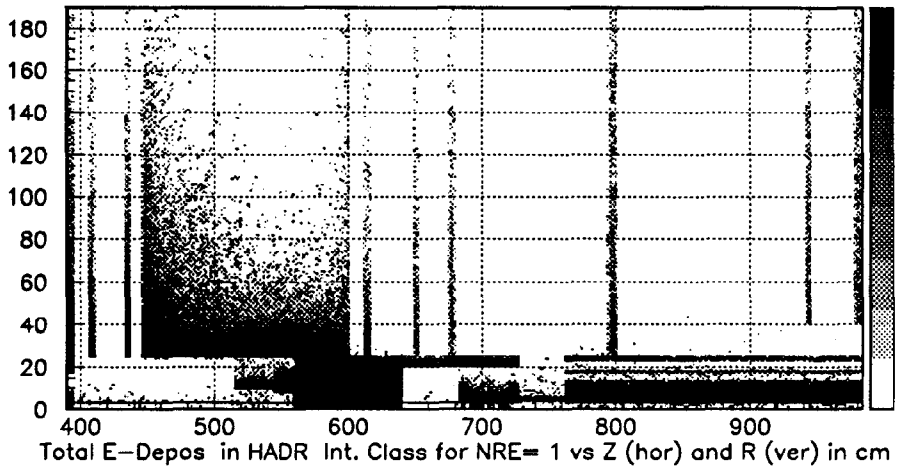

FIGURE 2. Energy deposition in the D0 forward muon spectrometer and in the Tevatron components, in units of $10^n GeV/cm^3$ per second, where the shade indicates the power n.

Recently a first-pass study [45] showed that the electromagnetic component of the backgrounds from $\mu \rightarrow e\nu\tilde{\nu}$ decays has the potential of killing the very attractive concept of a high-energy high-luminosity $\mu^+\mu^-$ collider unless there is significant suppression via various shielding and collimators in the detector vicinity. All simulations in the whole 80-m long inner triplet and in the detector were done with MARS, version 13(95). The simplified detector geometry used in the calculations is shown in Fig. 3.

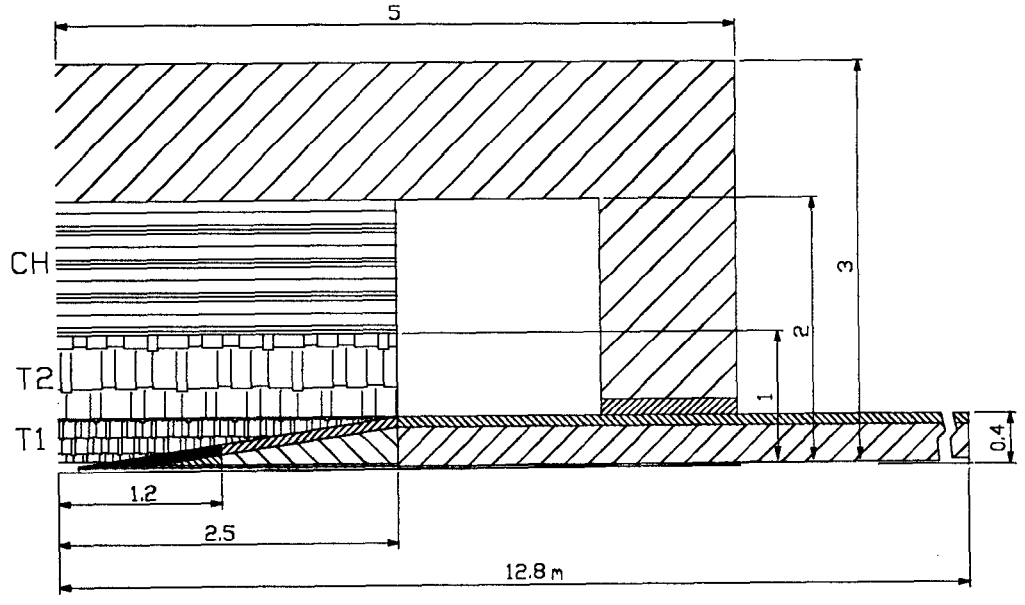

FIGURE 3. Detector, Q3 quadrupole and nozzle configuration used in the muon collider study. Dimensions are in meters.

In this application, MARS, allows an elegant way to handle the following processes:

- forced $\mu \rightarrow e\nu\tilde{\nu}$ decays in the beam pipe;
- tracking of created electrons in the beam pipe under influence of the magnetic field with emission of synchrotron photons along the track;
- simulation of electromagnetic showers in the triplet and detector components induced by electrons and synchrotron photons hitting the beam pipe;
- simulation of muon interactions (bremsstrahlung, direct e^+e^- pair production, ionization, deep inelastic nuclear interactions) and decays along the tracks in the lattice and detector;
- simulation of electromagnetic showers in the triplet and detector components created at the above muon interaction vertices;
- histogramming and analysis of particle energy spectra, fluences and energy deposition in various detector regions as well as in the whole IR.

Figure 4 shows calculated e^+e^- energy spectrum in the accelerator components in the vicinity of the detector. The huge peak sitting around 1 TeV represents the $\mu \rightarrow e\nu\tilde{\nu}$ decay spectrum with a tail at lower energies enriched by electrons and positrons of electromagnetic showers induced in the beam pipe and superconducting coils. Photons emitted due to synchrotron radiation along e^+e^- tracks in a strong 8 T magnetic field have an average energy around 1 GeV. The number of photons is about 300 times that for electrons and positrons.

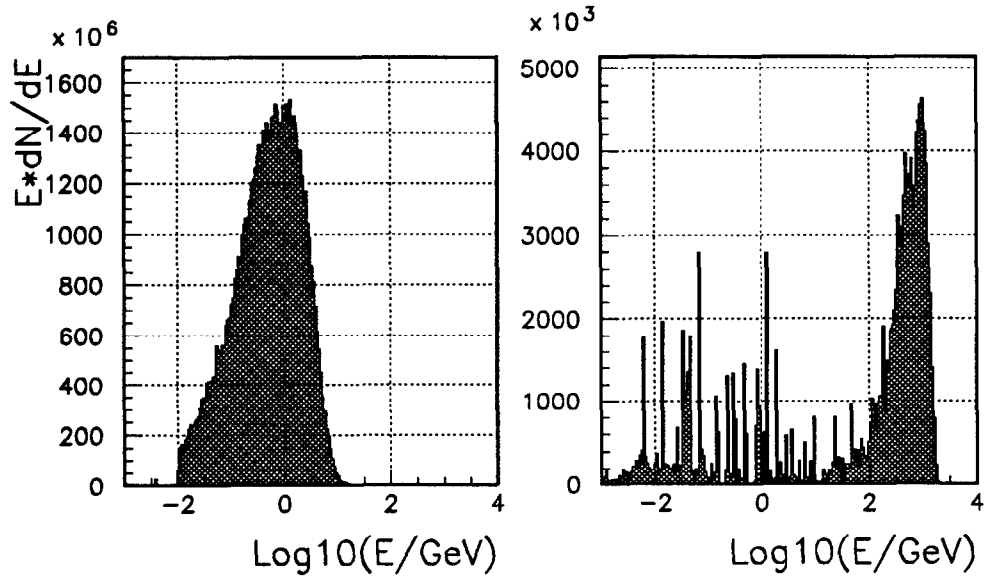

FIGURE 4. Photon (left) and electron/positron (right) energy spectra in the inner triplet accelerator components.

References for numerous comparisons of MARS code predictions with data and with other codes are given in Section 2.1. A few rather interesting recent comparisons are presented below. Figure 5 shows attenuation of a dose rate along the 30-inch waveguide conduit adjacent to a Linac tunnel where an accidental beam loss (70 MeV, 6×10^{13} protons per sec) takes place. The results obtained with MARS and LAHET [58] are in a pretty good agreement. It is worthwhile to notice that the LAHET code has one of the best physics model for the intermediate energy range (20 to 600 MeV). An arsenal of non-analog techniques and a very detailed geometry description are necessary in these calculations making the agreement even more remarkable.

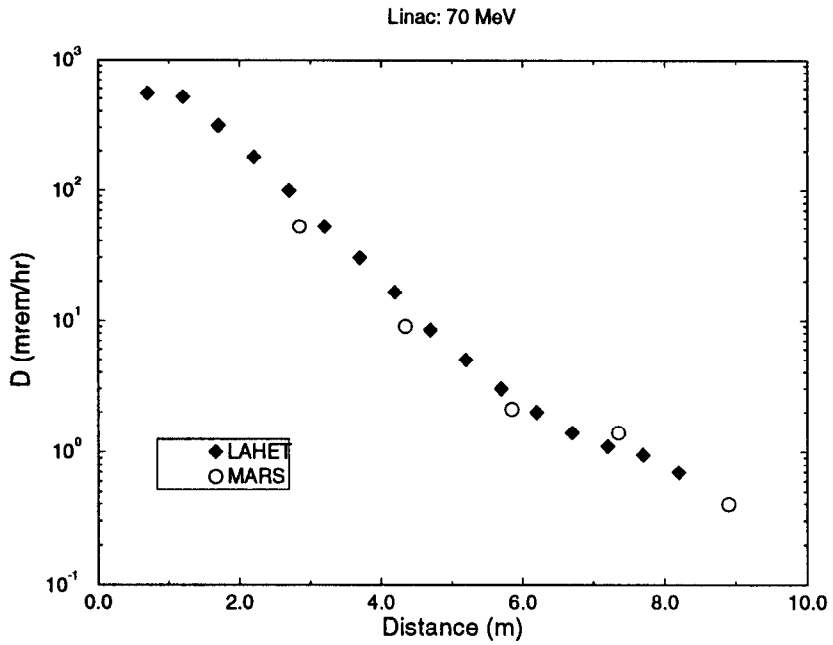

FIGURE 5. Dose rate along the Linac waveguides calculated with the LAHET (diamonds) and MARS (circles) codes.

Another example is a recent intercomparison of four popular codes for high energy hadronic cascades studies: FLUKA [13], LAHET [58], GCALOR (mariage of GEANT and CALOR codes) [59] and MARS. A simple configuration was chosen: 100-GeV proton beam irradiating a 3-m long iron cylinder ($\rho = 7.4 g/cm^3$) with a radius of 50 cm followed by 200 g/cm^2 of ordinary concrete ($\rho = 2.35 g/cm^3$). Table 11 gives the calculated total number of neutrons leaked through the front, side and back surfaces. Corresponding leakage neutron spectra calculated with FLUKA using its most sophisticated physics model and with MARS are also in a rather good agreement (Fig. 6).

Table 11 : Neutron leakage out of iron cylinder with a concrete shell.

Code	Front	Side	Back
MARS	153	4.2	0.96
FLUKA	118	3.6	1.02
LAHET	176	5.3	0.67
GCALOR	163	5.7	0.97

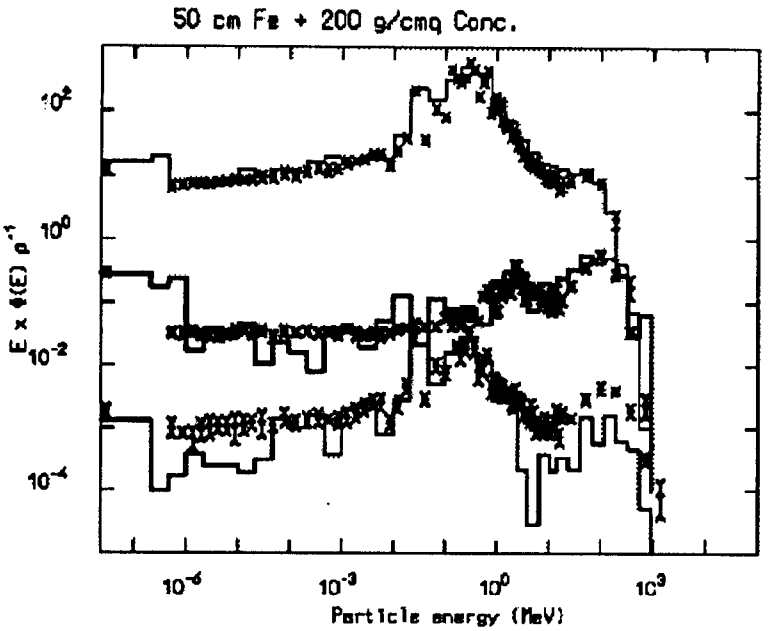

FIGURE 6. Neutron energy spectra leaked from the front (upper set, $\times 10$), side (middle set), and back (lower set, $\times 0.1$) of the shielding as calculated with the MARS (histogram) and FLUKA92 (symbols) codes.

Comparisons for cascades induced by 20-TeV proton beam loss along the superconducting magnets in the SSC tunnel are shown in Fig. 7. Neutron spectra in the tunnel cross-section, obtained with the FLUKA and MARS codes, agree very well in the energy range spanning 10 decades. MARS calculations are also in a good agreement with GCALOR and FLUKA92 predictions in designs of shield configurations to reduce the background rates in the GEM detector at the SSC [34] and in the CMS muon system for the LHC project [60].

It is worthwhile to notice a recent remarkable achievement with the D0 detector at Fermilab [54]. A system to suppress backgrounds in the forward muon spectrometer, designed with the help of MARS coupled with the STRUCT code, has been installed in the vicinity of the experimental hall and has provided substantial reduction of the accelerator related particle fluxes in the detector, in an excellent agreement with MARS predictions.

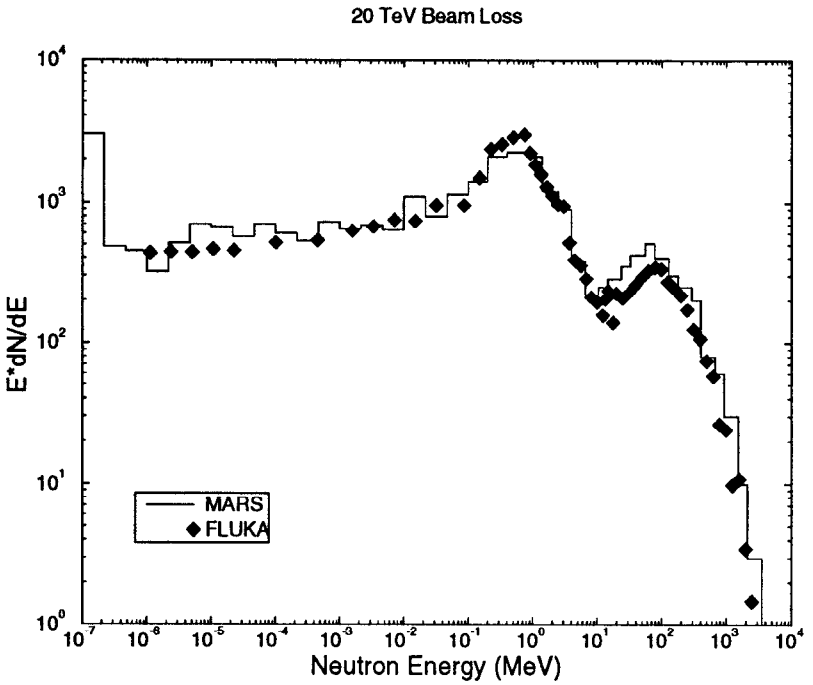

FIGURE 7. Neutron energy spectra ($cm^{-2} per 10^4 p/m$) in the SSC tunnel for the routine 20-TeV proton beam loss in the superconducting magnets, calculated with the MARS (histogram) and FLUKA92 (diamonds) codes.

7 Rules-Of-Thumb

It is obvious that the quality of the typical output of any code, for given physics model, depends on how the user built the calculational model and how he/she handled the code. The geometry description is of primary importance. Then, as stated above, the most essential parameters to control the calculational accuracy for given physics model are the number of incidents (primary events) NEVT and the accuracy of boundary localization in iterative transport algorithm STEPEM. Naturally, the higher NEVT and the smaller STEPEM, the better the result will be. But here we come to a conradiction with both CPU time t_1 and time t_2 alotted for the whole problem. The strategy would be to keep both t_1 and t_2 as small as possible. There are a few rules for a user to get the best from the MARS code. These rules are:

1. Required NEVT is determined by a statistical error in a phase-space or geometrical region of interest. The calculated results in a given region N are statistically valid only if a R.M.S. statistical error $\delta \leq 20\%$. So, run until this condition is satisfied. Do short runs first to estimate required NEVT and play with DUMP output.

2. Keep STEPEM$\simeq 0.3 \times t_{min}$, where t_{min} is a smallest linear size of the smallest region in the considered geometry.

3. Use as few as possible geometrical regions described in all the *standard*, *extended* and *user − supplied* sectors: CPU time grows almost linearly with the number of regions in the direction of predominant propagation of the particles.

4. Versions 13.1(95) and 13.2(95) are built such a way that in many typical applications they give identical results and only at very high energies (TeV region) and/or for very fine geometrical structures the user should use version 13.1(95) with `-r8` option.

5. Use `IND(6)=T` and DLEXP$\neq$1 options with a great care. Do short tests first.

6. Use `IND(8)=F` in a routine run to reduce amount of the output.

7. Use `IND(1)=F`, if you do not need energy deposition related distributions or photon and electron fluxes.

8. Use `IND(9)=F`, if you are not studying an extremely fine geometrical structure.

9. Use `IND(10)=F`, if you are not interested in muon production.

10. Use `IND(12)=F`, if you are not interested in antiproton production.

11. Use `IND(14)=F`, if you are not specificaly interested in low-energy neutron fluxes.

In the last five rules, the code takes care of those components in some effective manner anyway, but the user can reduce the CPU time drastically if he/she turns off the corresponding options.

8 Acknowledgements

I express my gratitude to S. I. Striganov, I. A. Kurochkin and V. V. Talanov for their contribution to this version of the MARS code. My thanks to A. Van Ginneken and F. Ostiguy for useful comments on this paper.

References

[1] N. V. Mokhov, "The MARS10 Code System: Inclusive Simulation of Hadronic and Electromagnetic Cascades and Muon Transport", *Fermilab FN-509* (1989).

[2] N. V. Mokhov, "The MARS12 Code System", in *Proceedings of the SARE Workshop*, Santa Fe, January 1993.

[3] P. Aurenche, F. Bopp, R. Engel, D. Pertermann, J. Ranft, and S. Roesler, "DTUJET93, Sampling Inelastic Proton-Proton and Proton-Antiproton Collisions According to the Two-Component Dual Parton Model", *SI-93-3* (1994).

[4] I. Baishev, A. Drozhdin, and N. Mokhov, "STRUCT Program User's Reference Manual", *SSCL-MAN-0034* (1994).

[5] R. P. Feynman, Phys. Rev. Lett., **23**, 1415 (1969).

[6] N. V. Mokhov, *Proc. IV All-Union Conference on Charged Particle Accelerators,* Moscow, "Nauka" **2**, 222 (1975); N. V. Mokhov and V. V. Phrolov, *Sov. J. Atomic Energy*, **38**, 226 (1975).

[7] A. Van Ginneken, "CASIM – Program to Simulate Transport of Hadronic Cascades in Bulk Matter", *Fermilab FN-272* (1975); "Weighted Monte Carlo Calculations in Thick Targets", *Fermilab FN-250* (1972).

[8] A. Van Ginneken, "Calculation of the Average Properties of Hadronic Cascades at High Energies (CASIM), in *Computer Techniques in Radiation Transport and Dosimetry*, W. R. Nelson and T. M. Jenkins Ed., Plenum, New York (1978).

[9] N. V. Mokhov, Sov. J. Part. Nucl., **18**(5), pp. 408-426 (1987).

[10] N. V. Mokhov, "Inclusive simulation of hadronic and electromagnetic cascades in the SSC components," in *Radiation Levels in the SSC Interaction Regions,* SSC Central Design Group Report SSC-SR-1033, pp. 303-311 (1988).

[11] A. N. Kalinovsky, N. V. Mokhov, and Yu. P. Nikitin, "Passage of High-Energy Particles through Matter", AIP, New York (1989).

[12] W. R. Nelson, H. Hirayama, and D. Rogers, "The EGS4 Code System", *SLAC-265* (1985).

[13] A. Fasso, A. Ferrari, J. Ranft, and P. Sala, "FLUKA92", in *Proceedings of the SARE Workshop*, Santa Fe, January 1993.

[14] N. V. Mokhov, S. I. Striganov, and A. V. Uzunian, *IHEP 87-59*, Serpukhov (1987).

[15] I. L. Azhgirey, N. V. Mokhov, and S. I. Striganov, "Antiproton Production for Tevatron", *Fermilab TM-1730* (1991).

[16] S. L. Kuchinin, N. V. Mokhov, and Ya. N. Rastsvetalov, *IHEP 75-74*, Serpukhov (1975).

[17] I. S. Baishev, S. L. Kuchinin, and N. V. Mokhov, *IHEP 78-2*, Serpukhov (1977).

[18] M. A. Maslov, and N. V. Mokhov, Particle Accelerators, **11**, 91 (1980).

[19] N. V. Mokhov, "Energy Deposition in Targets and Beam Dumps at 0.1-5 TeV Proton Energy", *Fermilab FN-328* (1980).

[20] N. V. Mokhov, *IHEP 82-168*, Serpukhov (1982).

[21] N. V. Mokhov, and J. D. Cossairt, Nucl. Instrum. Meth., **A244**, 349 (1986).

[22] I. S. Baishev, I. A. Kurochkin, and N. V. Mokhov, *IHEP 91-118*, Protvino (1991).

[23] I. L. Azhgirey, I. A. Kurochkin, M. A. Maslov, V. V. Talanov, and A. V. Uzunian, *IHEP 93-19*, Protvino (1993).

[24] D. C. Wilson, C. A. Wingate, J. C. Goldstein, R. P. Godwin, and N. V. Mokhov, "Hydrodynamic Calculations of 20-TeV Beam Interactions with the SSC Beam Dump", in *Proceedings of the 1993 Particle Accelerator Conference, IEEE*, pp. 3090-3092 (1993).

[25] J. Ftacnik, and M. Popovic, "Parallel Version of MARS10 and MARS12 Codes", *The 1994 April APS Meeting* (1994).

[26] N. V. Mokhov, and A. Van Ginneken, "Increasing Antiproton Yields via Recirculating Beam Targeting", *Fermilab FN-621* (1994).

[27] Yu. M. Shabelsky, Sov. J. Part. Nucl., **12**, 430 (1981).

[28] E. Stenlund, and I. Otterlund, *CERN-EP/82-42* (1982).

[29] J. Ranft, and J. T. Routti, Particle Accelerators, **4**, 101 (1972).

[30] J. Hansgen et al., *KMU-HEP-83-06* (1983).

[31] L. C. Tan, and L. K. Ng, J. Phys. G: Nucl. Phys., **9**, 1289-1308 (1983).

[32] B. S. Sychev, A. Ya. Serov, and B. V. Man'ko, *MRTI-799*, Moscow (1979).

[33] N. V. Mokhov, "Accelerator-Experiment Interface at Hadron Colliders: Energy Deposition in the IR Components and Machine Related Background to Detectors", *FERMILAB-Pub-94/085* (1994).

[34] M. Diwan, Y. Fisyak, N. Mokhov et al., "Radiation Environment and Shielding for the GEM Experiment at the SSC", *SSCL-SR-1223* (1993).

[35] S. I. Striganov, *IHEP 94-14* (1994).

[36] L. P. Abagyan, N. O. Bazazyants, M. N. Nikolaev, and A. M. Tsybulya, "Group Cross-Sections for Reactor and Shielding Calculations", Moscow, Energoizdat (1981).

[37] I. Baishev, N. Mokhov, and T. Toohig, "The SSC Access Shafts Calculational Study", *SSCL-496* (1991); I. Baishev, and N. Mokhov, "Firming Up the SSC Access Shafts Calculations", *SSCL-521* (1992).

[38] R. Meinke, N. Mokhov, D. Orth, B. Parker, and D. Plant, "Radiation Shielding for the Super Collider West Utility Region", *SSCL-663* (1994); also in *Proceedings of 8th Int. Conference on Radiation Shielding*, pp. 1008-1014, Arlington, Texas, April 24-28 (1994).

[39] I. S. Baishev, N. V. Mokhov, and S. I. Striganov, Sov. J. Nucl. Physics, **42**, 1175 (1985).

[40] A. I. Drozhdin, M. Harrison, and N. V. Mokhov, "Study of Beam Losses During Fast Extraction of 800 GeV Protons from the Tevatron", *Fermilab FN-418* (1985).

[41] Striganov, S., *Nucl. Instruments and Methods*, **A322**, 225-230 (1992); "Fast Precise Algorithm for Simulation of Ionization Energy Losses", *IHEP 92-80*, Protvino (1992).

[42] I. S. Baishev, *IHEP 87-149*, Serpukhov (1987).

[43] N. V. Mokhov, G. I. Semenova, and A. V. Uzunian, Nucl. Instrum. Meth., **180**, 469 (1981).

[44] M. A. Maslov, N. V. Mokhov, and A. V. Uzunian, *Nucl. Instruments and Methods*, **217**, 419 (1983).

[45] G. W. Foster, and N. V. Mokhov, "Backgrounds and Detector Performance at a 2×2 TeV $\mu^+\mu^-$ Collider", *Fermilab-Conf-95/037* (1995); to be published by AIP in *Proceedings of the 2nd Workshop on Physics Potential and Development of $\mu^+\mu^-$ Colliders*, Sausalito, California, November 17-19, 1994.

[46] B. L. Berman, and S. C. Fultz, Rev. Mod. Phys., **47**, 713 (1975).

[47] A. Van Ginneken, "AEGIS – a Program to Calculate the Average Behavior of Electromagnetic Showers", *Fermilab FN-309* (1978).

[48] I. S. Baishev, M. A. Maslov, and N. V. Mokhov, in *Proc. VIII All-Union Conference on Charged Particle Accelerators*, Dubna, **2**, 167 (1983).

[49] M. A. Maslov, and N. V. Mokhov, *IHEP 85-8*, Serpukhov (1985).

[50] V. V. Talanov, *IHEP 92-99*, Protvino (1992).

[51] I. S. Baishev, A. I. Drozhdin, and N. V. Mokhov, "Beam Loss and Radiation Effects in the SSC Lattice Elements", *SSCL-306* (1990).

[52] A. Drozhdin, N. Mokhov, R. Soundranayagam, and J. Tompkins, "Toward Design of the Collider Beam Collimation System", *SSCL-Preprint-555* (1994).

[53] A. Drozhdin, N. Mokhov, and B. Parker, "Accidental Beam Loss in Superconducting Accelerators: Simulations, Consequences of Accidents and Protective Measures", *SSCL-Preprint-556* (1994).

[54] J. M. Butler, D. S. Denisov, H. T. Diehl, A. I. Drozhdin, N. V. Mokhov, and D. R Wood, "Reduction of Tevatron and Main Ring Induced Backgrounds in the D0 Collision Hall", *Fermilab FN-629* (1995).

[55] R. Brun, and D. Lienart, "HBOOK User Guide", *CERN Program Library Y250.*

[56] R. Brun, O. Couet, C. Vandoni, and P. Zanarini, "PAW Physics Analysis Workstation", *CERN Program Library Q121.*

[57] G. Marsaglia, and A. Zaman, "Toward a Universal Random Number Generator", *FSU-SCRI-87-* (1988).

[58] R. E. Prael, and H. Lichtenstein, "LAHET Code System", *LA-UR-89-3014* (1989).

[59] C. Zeitnitz, and T. A. Gabriel, "GCALOR", in *Proceedings of the SARE Workshop*, Santa Fe, January 1993; *Nucl. Instruments and Methods*, **A349**, 106 (1994).

[60] "The Compact Muon Solenoid", Technical Proposal, *CERN/LHCC 94-38*, December 1994.